Proceedings 10th NUMGE 2023
10th European Conference on Numerical Methods in Geotechnical Engineering
Zdravkovic L, Kontoe S, Taborda DMG, Tsiampousi A (eds)

https://doi.org/10.53243/NUMGE2023-271

Floating offshore wind turbine piles under horizontal cyclic loading: calibration and performance of advanced soil constitutive models

R. Chalhoub, O. Jenck, C. Dano

Grenoble Alpes University, CNRS, Grenoble INP, 3SR, Grenoble, France

ABSTRACT: Driven by the demand for renewable energies, the development of floating offshore wind turbines (FOWT) has recently raised significant interest, as stronger and more consistent wind currents can be reached with less space constraints. In a previous study, the behaviour of steel piles, used as a solution to anchor FOWT, was numerically investigated, but it was concluded that relatively simple elastoplastic models are not able to properly capture the soil behaviour under multi-directional lateral loadings. Here, three different constitutive models (Mohr-Coulomb, CHSoil and SANISAND) are briefly presented and calibrated based on experimental data found in the literature. Then, a pile founded in dense homogeneous sand is modelled using a three-dimensional finite volume program. The performances of the different models are compared for a specific case in which the pile is subjected to mono-directional lateral cyclic loading as a preliminary investigation of its response under multi-directional loading. The results show that the SANISAND model exhibits a more realistic evolution of the pile head displacement compared to the two more simplistic models.

Keywords: Numerical Modelling; Offshore Wind Turbine; Pile; Cyclic Lateral Loading; SANISAND

1 INTRODUCTION

Over the past two centuries, the large amount of greenhouse gases released by burning fossil fuels has been the main driver of climate change. With the expected rise of energy consumption due to the globally expanding access to electricity, switching energy systems from fossil fuels to renewables is a major step toward the decarbonization of electrical power.

Wind energy has established itself as a major source of environmentally-friendly renewable energy (Sheil and McCabe, 2016). Recently, the development of offshore wind turbines has raised significant interest. More specifically, floating wind turbines show a great advantage for deep waters, where bottom-fixed foundations can no longer be used. In this way, each turbine should be connected to multiple anchors in order to guarantee its stability. These anchors will be subjected to cyclic, alternate, and most importantly multi-directional loadings.

While the pile-soil behaviour subjected to mono-directional loading is relatively well understood (Puech and Garnier, 2017), the number of studies considering multi-directional loading documented in the literature is limited. Sheil and McCabe (2016) conducted a numerical study on the mechanical behaviour of a pile under multi-directional loading using two different constitutive soil models: a hypoplastic model and the elastoplastic hardening soil model with small-strain stiffness (HSsmall). They concluded that the results were heavily dependent on the adopted soil model and that the HSsmall model was only suitable for mono-directional loading since it led to non-conservative predictions in the case of multi-directional loading. A similar study was conducted by Jenck et al. (2021) using two relatively simple elastoplastic soil models. In that work, several loading cases were considered, and mono-directional and multi-directional cyclic loadings were applied on the pile under the same conditions. One of the main conclusions was that a complex constitutive model should be used in order to capture the key aspects of the mechanical response of the soil.

Hence, in this paper, the shortcomings of these models are addressed through the introduction of a more complex one: the SANISAND model developed by Dafalias and Manzari (2004). It is calibrated and tested along with two other elastoplastic models: the linear elastic perfectly plastic model with Mohr-Coulomb failure criterion, simply referred to as “Mohr-Coulomb” hereafter and the Simplified Cap-Yield (CHSoil) model. Then the pile-soil behaviour is studied under mono-directional cyclic loading and compared to the results found in the literature, as a preliminary investigation before applying the multi-directional loadings.

The program used is FLAC3D (Fast Lagrangian Analysis of Continua in 3 dimensions) version 7.0 (Itasca, 2019), which is an explicit finite volume program widely used in geotechnical engineering.

2 SOIL CONSTITUTIVE MODELS AND PARAMETER CALIBRATION

In this section, brief descriptions of the three constitutive models are presented, as well as their calibration procedures based on available experimental data on Fontainebleau NE34 sand, a reference sand in France. The NE34 is a fine silica sand that consists of sub-rounded to rounded grains (mean grain size d_{50} = 210 µm; coefficient of uniformity C_u = 1.4). It has a maximum void ratio of 0.87, a minimum void ratio of 0.53, and a specific gravity of 2.65.

2.1 Theory and calibration procedures

2.1.1 Mohr-Coulomb

The calibration of the parameters of this model can be easily performed, by dealing with it as a simplified version of the CHSoil model, described in the next section. Therefore, the same values of the strength parameters (friction angle and cohesion), the dilation angle and Poisson's ratio, resulting from the calibration of CHSoil are used for Mohr-Coulomb. The main difference between Mohr-Coulomb and CHSoil is that for the latter, the stiffness is stress dependent. Consequently, for each soil state, the Young's modulus value for Mohr-Coulomb is considered as the average of the values determined for different confining pressures, at this state, using CHSoil. The values are then 400 MPa, 200 MPa and 112 MPa for the dense, medium-dense and loose samples, respectively.

2.1.2 CHSoil

The CHSoil soil model is considered as an alternative to the model developed by Duncan and Chang (1970) (Itasca, 2019). This model includes a built-in friction hardening law to capture non-linear stress-strain behavior, and a Mohr-Coulomb shear envelope. The parameter calibration procedure presented here is inspired by the one developed by Santacruz Reyes (2017), for a modified version of CHSoil. In order to obtain the model parameter values directly from triaxial data, Santacruz Reyes (2017) recasted the CHSoil formulation by correlating deviatoric stress to axial strains as well as volumetric strains to axial strains. The calibration procedure of the original CHSoil model consists of the five following steps that are applied for each state of the soil:

Step 1: Determine the ultimate friction angle ϕ_f.
By assuming the cohesion is zero, the ultimate friction angle can be obtained using the maximum deviatoric stress ($\sigma_{d,f}$) and the confining stress (σ_3) (Equation (1)).

$$\phi_f = sin^{-1}\left(\frac{\sigma_{d,f}}{\sigma_{d,f}+\sigma_3}\right) \quad (1)$$

Step 2: Determine the dilation angle and bulk modulus. The dilation angle is calculated using the axial and volumetric strain increments when the maximum deviator stress is reached. As shown in Equation (2), the elastic bulk modulus K^e is the initial ratio of the deviator stress variation over three times its corresponding volumetric strain variation.

$$K^e = \frac{\Delta\sigma_d}{3\Delta\varepsilon_v} \quad (2)$$

Step 3: Determine the shear modulus and failure ratio.
Step 4: Repeat Steps 1, 2 and 3 for the different confining pressure values for each soil state.
Step 5: Estimate the parameters for each sand state.
The small strain elastic shear and bulk moduli are functions of the initial mean effective stress according to Equations (3-4) respectively.

$$G = G_{ref}\, p_{ref}\left(\frac{p'_m}{p_{ref}}\right)^n \quad (3)$$

$$K = K_{ref}\, p_{ref}\left(\frac{p'_m}{p_{ref}}\right)^m \quad (4)$$

where p_{ref} is the reference pressure (atmospheric pressure) and p'_m is the initial confining pressure. K_{ref} and G_{ref} are estimated by fitting these equations to the results calculated in the previous steps assuming $m = n$ = 0.5. As for the rest of the parameters, the averages of the values for each state are considered.

Table 1. Parameters of the CHSoil model for Fontainebleau NE34 sand

Parameter	Physical meaning	Dense	Medium	Loose
E_{ref}	Young's modulus number	3107	2350	874
ν	Poisson's ratio	0.2	0.2	0.2
Ψ [°]	Maximum dilation angle	10	6.6	2.8
m	Bulk modulus exponent	0.5	0.5	0.5
n	Shear modulus exponent	0.5	0.5	0.5
ϕ_f [°]	Ultimate friction angle	40	37	34
R_f	Failure ratio	0.92	0.92	0.94
c [kPa]	Cohesion	0	0	0

2.1.3 SANISAND

The term SANISAND is the acronym for Simple ANIsotropic SAND, used to identify the family of constitutive models developed over the past two decades based on the original two-surface plasticity model developed by Manzari and Dafalias (1997). The model is formulated based on the bounding surface plasticity and is able to realistically simulate the granular material behavior under conventional monotonic and cyclic loading paths. Many extensions were introduced over the years, in order to overcome some model's limitations (Dafalias and Manzari, 2004; Taiebat et al. , 2010). All these models have the advantage to use a unique set of model parameters for any initial void ratio or confining pressure for a given sand, as well as to distinguish dense samples from loose ones. The SANISAND model used in this study was developed by Dafalias and Manzari (2004), in order to account for the effect of the change in fabric during reverse loading, which improved the model capability under cyclic loading. This model was implemented as a user-defined model in the FLAC3D environment by Cheng et al. (2013).

The calibration procedure used in this work is based on several procedures found in the literature (Taiebat et al. , 2010; Latini, 2018; Roy, 2021). The parameters are calibrated in the following order. First, for the elastic part of the model, the isotropic hypo-elasticity is adopted. The elastic shear modulus G is considered as a function of the effective mean pressure p' and the current void ratio e (Richart et al., 1970) as:

$$G = G_0\, p_{atm}\, \frac{(2.97-e)^2}{1+e} \left(\frac{p\prime}{p_{atm}}\right)^{1/2} \qquad (5)$$

where p_{atm} is the atmospheric pressure for normalization. The G_0 parameter is calibrated based on shear wave propagation tests along isotropic stress paths performed on Fontainebleau sand (Dano, 2001). Poisson's ratio was assigned an arbitrary value between 0.1 and 0.3 as an initial guess, which will be refined at the end in order to reproduce a proper stress-strain fit for all the data sets. Then the critical state line parameters in the $e-p$ plane (e_0, λ and ξ) were calibrated based on drained and undrained triaxial tests data from Altuhafi et al. (2018) and Aghakouchak (2015). In fact, the critical void ratio e_c is related to the critical pressure p_c by the following power relation (Li and Wang, 1998):

$$e_c(p_c) = e_0 - \lambda \left(\frac{p_c}{p_{atm}}\right)^{\xi} \qquad (6)$$

e_0 and λ are obtained by fitting this equation to the abovementioned data assuming $\xi = 0.6$, which gives the best fit to the data, among the values usually considered in the literature. The critical state stress ratio M is the ratio $(q/p)_{critical}$ at which the soil deforms continuously in shear at fixed stresses with zero volumetric strain rate. The undrained triaxial tests on very loose NE34 sand samples performed by Benahmed (2001) allow for an accurate estimation of this parameter. Next, the parameter m that controls the size of the yield surface cone, is usually set to about 1/100 M, so that plastic strain can develop almost immediately after the application of shearing. As for the parameters related to the dilatancy and plastic modulus, the values reported in the literature for the NE34 sand were considered as a primary estimation and were then refined by trial and error, for an overall good fit of the curves from drained triaxial tests. Finally, the values of fabric dilatancy parameters c_z and z_{max} used by Dafalias and Manzari (2004) gave a good estimation of the undrained cyclic triaxial tests. The final values of the calibrated dimensionless model parameters are listed in Table 2.

Table 2. Parameters of the SANISAND model for Fontainebleau NE34 sand

Parameter		Physical meaning	Value
Elasticity	G_0	Constant of elastic shear modulus	299.5
	ν	Poisson's ratio	0.12
Critical state line	M	Critical stress ratio	1.26
	c	Ratio of extension to compression strength	0.77
	λ	Slope of the critical state line in e−p plane	0.021
	e_0	Intercept of the critical state line in e− p plane	0.782
	ξ	Exponent of the critical state line in e− p plane	0.6
Yield surface	m	Tangent of half the opening angle of the yielding surface	0.01
Plastic modulus	h_0	Constant of hardening modulus H	4
	c_h	Constant of hardening modulus H	0.96
	n^b	Material constant to calculate the stress image on the boundary surface	1.95
Dilatancy	A_0	Dilatancy constant	0.65
	n^d	Material constant to calculate the stress image on the dilatancy surface	1.5
Fabric dilatancy	c_z	Control of the pace evolution of z	600
	z_{max}	Maximum value that z can attain	4

2.2 *Validation by comparison to laboratory tests*

Figure 1 compares drained triaxial compression tests simulated using the three constitutive models, and laboratory tests performed by Andria-Ntoanina et al. (2010) on dense NE34 sand samples (e_0=0.537), at four different values of initial confining pressure. Other series of tests were also simulated in the case of medium-dense and loose samples, but will not be presented here. Although the slight difference in the volumetric strain curves exhibited by the SANISAND model, this latter allows for an overall better simulation of the sand behaviour, especially the post-peak softening which can not be captured by the other models.

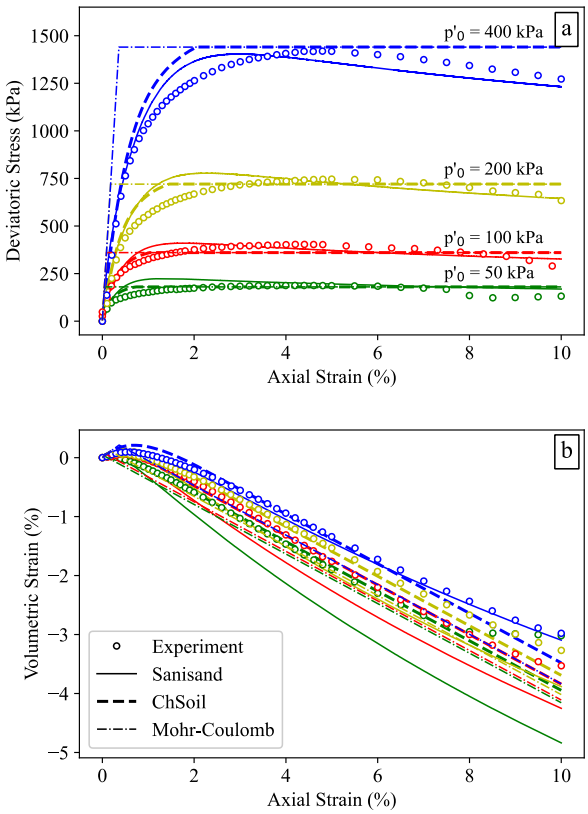

Figure 1. Comparison between simulations and experiments of drained triaxial tests from Andria-Ntoanina et al. (2010). (a) stress:strain response; (b) volumetric strain response

Andria-Ntoanina (2011) carried a series of undrained cyclic triaxial tests on medium-dense and loose Fontainebleau NE34 samples, both under symmetric and asymmetric loading. The results shown in Figure 2 correspond to a medium-dense sample under symmetric loading with cyclic amplitude q_{cyc} = 40 kPa and an initial mean stress p'_0 = 200 kPa. Unlike CHSoil and Mohr-Coulomb, the SANISAND model is able to capture a "butterfly-shaped" stress path and a cyclic shear strain accumulation. These results along with other results for undrained triaxial tests show that the SANISAND model captures the overall trend and is able to simulate the cyclic behaviour relatively well.

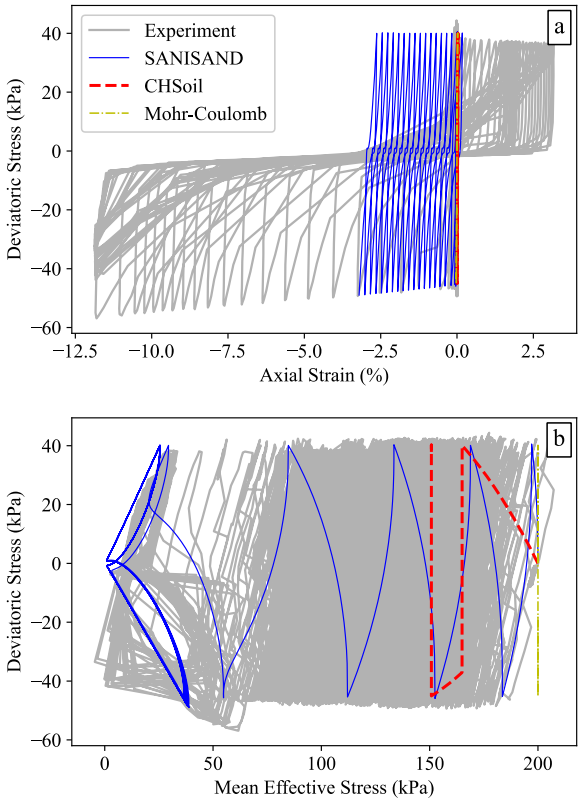

Figure 2. Comparison between simulations and experiments of cyclic undrained triaxial tests from Andria-Ntoanina (2011). (a) stress-strain relations; (b) effective stress path

3 CYCLIC BEHAVIOUR OF PILE-SOIL FOUNDATION

3.1 *Modelling procedure*

The main features of the numerical model are based on a previous numerical study to assess FOWT anchor pile behaviour under multi-directional cyclic loading (Jenck et al., 2021). The model components are threefold (Figure 3):

1. A 10m long hollow steel cylinder pile of diameter D = 1.7m, simulated as a solid cylinder for the sake of model simplicity. An equivalent bending stiffness value ($E_p \times I_p$) is assigned to it in order to take this assumption into consideration. Additionally, a beam of low characteristics is implemented along the pile axis in order to easily calculate the generated bending moments.
2. A homogeneous dense sand mass in which the pile is embedded, of 30 D = 51m width and 17.85m height. The applied boundary conditions consist of fixing the nodes in the x and y directions for the vertical planes perpendicular to the x and y directions, respectively. As for the bottom plane, the nodes are fixed in all directions. The coefficient of earth at rest K_0 is calculated based on Jaky's equation (K_0 = 0.389 with ϕ = 40°).

3. An interface between the pile and the surrounding soil using the standard interface feature from the software. The interface elements are characterized by a normal stiffness (k_n = 1200 kPa/mm), a shear stiffness (k_s = 1200 kPa/mm), an interface friction angle (ϕ_{int} = 2/3 ϕ), and a cohesion (c_{int} = 0 kPa).

Only half of the model is simulated, taking advantage of the symmetry in the case of mono-directional loading.

In order to apply a load on the pile head, a velocity is applied to the corresponding grid-points and servo functions compute the resulting force and adapt the applied velocity. In this way, a monotonic loading along the x-axis is first applied on the pile head until reaching the maximum horizontal force H_{max} = 1.77 MN, followed by a series of 20 cycles between H_{max} and H_{min} = 1.25 MN. The choice of the number of cycles is justified by the fact that the overall behaviour is governed by the first few dozen cycles (Puech and Garnier, 2017).

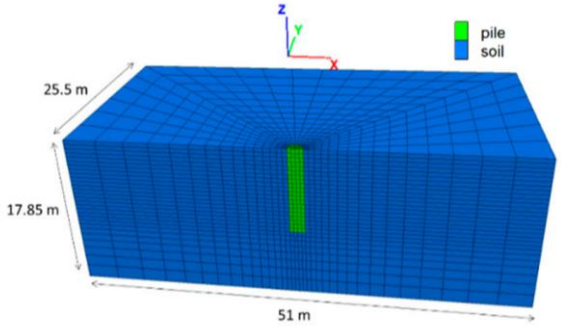

Figure 3. Numerical model for mono-directional loading (Jenck et al., 2021)

3.2 Results

The analysis in this section mainly consists in determining the lateral displacement of the pile head during the cyclic loading, as well as the evolution of the bending moment in the pile.

Figure 4 presents the lateral force developed at the pile head according to its displacement. Unlike Mohr-Coulomb and CHSoil, the large displacement accumulations obtained using the SANISAND model are due to its capacity of modelling the strain accumulation during the cycles as explained in the previous section.

In order to evaluate the lateral displacement accumulation during the cycles, Lin and Liao (1999) proposed the following logarithmic law based on field-scale piles:

$$y_N/y_1 - 1 = \alpha \ln(N) \quad (N \geq 1) \qquad (7)$$

where y_1 and y_N are the pile head lateral displacements at the first and Nth cycle respectively, and α is the degradation parameter that represents the displacement accumulation due to the cycles.

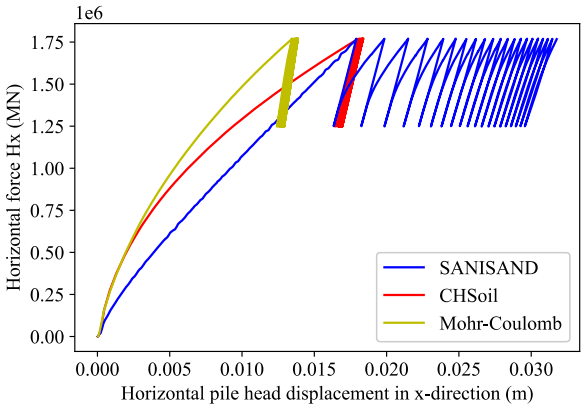

Figure 4. Force displacement curves using the three different soil constitutive models

In order to estimate the value of α, the data obtained using the different models are fitted using Equation (7). The value of this parameter obtained using the SANISAND model, lies in the range of values presented by Puech and Garnier (2017) ($0.04 \leq \alpha \leq 0.25$), however, the other models result in very small values of α (Figure 5). Even though this law does not accurately fit the data, it was only used for the sake of comparison, which cannot be made in a straightforward manner, since the experiments that led to these values were conducted in very diverse conditions (different levels of cyclic loading, variable number of cycles, different natures of cyclic loading…).

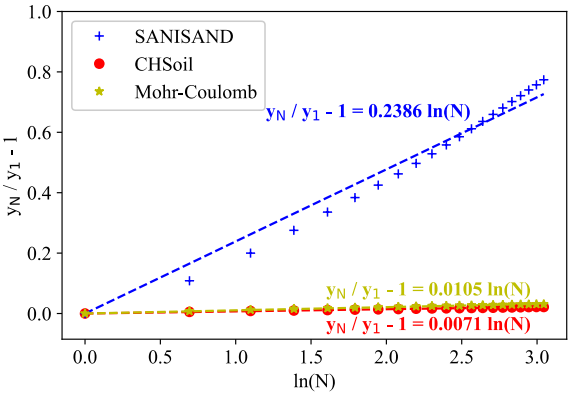

Figure 5. Accumulation of pile head displacement during the cycles and linear approximation with the logarithmic law

Figure 6 shows 18% increase in the maximum moment between the first and the 20th cycle using SANISAND, and an increase in its depth from -4.25 m to -4.75 m. While on the contrary, no significant evolution of the bending moment profile is detected for the other two models. Furthermore, many authors show that the evolution of the ratio $M_{max,N}/M_{max,1}$ with the number of cycles N can be accurately expressed by the following logarithmic function:

$$M_{max,N}/M_{max,1} - 1 = \mu \ln(N) \qquad (8)$$

where $M_{max,1}$ and $M_{max,N}$ are the maximum moments at the first loading and at the Nth cycle respectively. The

parameter μ = 0.074 and the percentage of increase in the maximum moment obtained using SANISAND are close to the ones reported in the literature, contrary to the very small values obtained using the elastoplastic models. This proves that SANISAND allows to better simulate the load transfer to the deeper layers of the soil.

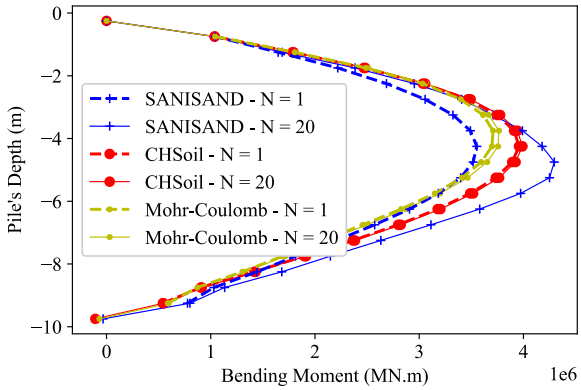

Figure 6. Pile bending moment profiles for the first and 20th cycles

4 CONCLUSIONS

In this paper, the behaviour of the foundation of a FOWT under cyclic lateral loading is studied.

The purpose was to assess the potential of using an advanced elastoplastic constitutive model, over two relatively simple elastoplastic models used in a previous study (Mohr-Coulomb and CHSoil). Consequently, the bounding surface plasticity model SANISAND was chosen to model the sand layer. The calibration procedures developed for each of the three models on the Fontainebleau NE34 sand were first presented.

On the laboratory scale, the SANISAND shows a better performance than the simpler elastoplastic models, for both monotonic and cyclic loadings, under drained and undrained conditions. This then results in a better performance of the SANISAND in simulating the FOWT foundation behaviour under cyclic mono-directional loadings. The accumulations of pile head displacements and the increase in the maximum moment developed in the pile are close to the values reported in the literature for similar loading cases.

The aim of this study was to first focus on the mono-directional cyclic loading, before simulating the multi-directional cyclic loading, which is the global objective of this research work. In a future study, this will be achieved by applying a multidirectional cyclic loading on the pile, with the above calibrated SANISAND as a constitutive model for the soil mass surrounding it.

5 ACKNOWLEDGEMENTS

The authors are grateful to the French Ministry for Higher Education and Research for providing financial support and for France Energies Marines for providing the framework of the case study.

6 REFERENCES

Aghakouchak A. 2015. Advanced laboratory studies to explore the axial cyclic behaviour of driven piles. *Ph.D Thesis*. Imperial College of London.

Altuhafi, F. N., Jardine, R. J., Georgiannou, V. N., Moinet, W. 2018. Effects of particle breakage and stress reversal on the behaviour of sand around displacement piles. *Géotechnique*, **68**, 546–555.

Andria-Ntoanina, I. 2011. Caractérisation dynamique de sables de référence en laboratoire. Application à la réponse sismique de massifs sableux en centrifugeuse. *Ph.D Thesis*, Université Paris Est.

Andria-Ntoanina I., Canou J. & Dupla JC. 2010. Caractérisation mécanique du sable de Fontainebleau NE34 à l'appareil triaxial sous cisaillement monotone. Report SOLCYP project.

Benahmed N. 2001. Comportement mécanique d'un sable ous cisaillement monotone et cyclique : application aux phénomènes de liquéfaction et mobilité cyclique. *Ph.D Thesis*, École Nationale des Ponts et Chaussées.

Cheng, Z., Dafalias, Y., Manzari, M. 2013. Application of SANISAND Dafalias-Manzari model in FLAC3.

Dafalias, Y. F., Manzari, M. T. 2004. Simple Plasticity Sand Model Accounting for Fabric Change Effects. *Journal of Engineering Mechanics* **130**, 622–634.

Dano C. 2001. Comportement mécanique des sols injectés. *Ph.D Thesis*, Ecole Centrale de Nantes.

Duncan, J. M., Chang, C. Y. 1970. Nonlinear Analysis of Stress and Strain in Soils. *Journal of the Soil Mechanics and Foundations Division*, **96**, 1629–1653.

Itasca Consulting Group Inc. 2019. Flac3D User's Guide, v.7.0. Minneapolis, MN, USA.

Jenck, O., Obaei, A., Emeriault, F., Dano, C. 2021. Effect of Horizontal Multidirectional Cyclic Loading on Piles in Sand: A Numerical Analysis. *Journal of Marine Science and Engineering*, **9**, 235–257.

Latini, C. 2018. Numerical modelling of offshore foundations for jacket structures. *Ph.D Thesis*, Technical University of Denmark.

Li, X.S., Wang, Y. 1998. Linear Representation of Steady-State Line for Sand. *Journal of Geotechnical and Geoenvironmental Engineering,* **124**, 1215–1217.

Lin, S., Liao, J. 1999. Permanent strains of piles in sand due to cyclic lateral loads. *Journal of Geotechnical and Geoenvironmental Engineering,* **125**, 798–802.

Manzari, M. T., Dafalias, Y. F. 1997. A critical state two-surface plasticity model for sands. *Géotechnique*,**47**,255–272.

Puech, A., Garnier, J. 2017. *Design of Piles under Cyclic Loading, SOLCYP Recommendations*, ISTE Editions, UK.

Roy, A. 2020. Numerical and experimental investigation of plate anchor capacity in sand. *Ph.D Thesis.* The University of Western Australia.

Santacruz Reyes, K. 2017. Geosynthetic Reinforced Soil: Numerical and Mathematical Analysis of Laboratory Triaxial Compression Tests. *Ph.D Thesis.* State University.

Sheil, B., McCabe, B. 2016. Biaxial loading of offshore monopiles: numerical modeling. *International Journal of Geomechanics*, **17**.

Taiebat, M., Jeremić, B., Dafalias, Y. F., Kaynia, A. M., Cheng, Z. 2010. Propagation of seismic waves through liquefied soils. *Soil Dynamics and Earthquake Engineering*, **30**, 236–257.